Ab initio density functional theory investigation of crystalline bundles of polygonized single-walled silicon carbide nanotubes

2008 J. Phys.: Condens. Matter 20 465214

(http://iopscience.iop.org/0953-8984/20/46/465214)

IOP PUBLISHING JOURNAL OF PHYSICS: CONDENSED MATTER

J. Phys.: Condens. Matter **20** (2008) 465214 (5pp) doi:10.1088/0953-8984/20/46/465214

Ab initio density functional theory investigation of crystalline bundles of polygonized single-walled silicon carbide nanotubes

Rostam Moradian[1,2,3], Somayeh Behzad[1] and Raad Chegel[1]

[1] Physics Department, Faculty of Science, Razi University, Kermanshah, Iran
[2] Nano Science and Technology Research Center, Razi University, Kermanshah, Iran
[3] Computational Physical Science Research Laboratory, Department of Nano Science, Institute for Studies in Theoretical Physics and Mathematics (IPM), PO Box 19395-5531, Tehran, Iran

E-mail: moradian.rostam@gmail.com

Received 20 August 2008, in final form 26 September 2008
Published 21 October 2008
Online at stacks.iop.org/JPhysCM/20/465214

Abstract

By using *ab initio* density functional theory, the structural characterizations and electronic properties of two large-diameter (13, 13) and (14, 14) armchair silicon carbide nanotube (SiCNT) bundles are investigated. Full structural optimizations show that the cross sections of these large-diameter SiCNTs in the bundles have a nearly hexagonal shape. The effects of inter-tube coupling on the electronic dispersions of large-diameter SiCNT bundles are demonstrated. By comparing the band structures of the triangular lattices of (14, 14) SiCNTs with nearly hexagonal and circular cross sections we found that the polygonization of the tubes in the bundle leads to a further dispersion of the occupied bands and an increase in the bandgap by 0.18 eV.

(Some figures in this article are in colour only in the electronic version)

1. Introduction

Since the discovery of carbon nanotubes (CNTs) by Iijima in 1991 [1], an extensive research field in the nanoscale area opened up due to their exceptional electronic, mechanical, thermal and transport properties. CNTs exist in several forms, from individual single-walled and multi-walled tubes to carbon nanotube bundles. Electronic properties of single-walled carbon nanotubes (SWCNTs) depend on their geometrical structures. An SWCNT can be constructed by rolling up a graphene sheet along a vector with specified direction which is called a chiral vector. Single-walled carbon nanotubes are semiconductors (or metals) when $n - m$ in their chiral vector (n, m) is not a multiple of 3 (when $n - m$ is a multiple of 3) [2]. The semiconducting energy gap in the semiconducting SWCNTs depends on the nanotube diameter [3]. Electronic properties of multi-walled carbon nanotubes (MWCNTs) could be different from the individual single walls [4].

Recently, silicon carbide nanotubes (SiCNTs) were synthesized via the reaction of silicon with MWCNTs at different temperatures [5]. The structure and stability of SiC nanotubes have been investigated using *ab initio* density functional theory in detail [6, 7]. It was found that SiC nanotubes with alternating Si–C bonds are more stable than the forms which contain C–C or Si–Si bonds [6]. While CNTs have been found to be either metallic or semiconducting, depending on their diameter and chirality, these calculations show that all the SiCNTs are semiconductors. The energy bandgap of the SiCNTs is dependent on their diameter and chirality, with direct gaps for zigzag tubes and indirect gaps for armchair and chiral tubes [6, 7]. This is due to the difference in the electronegativity of Si and C atoms, leading to the ionicity of Si–C bonds in the SiCNTs which localizes the electronic states. Carbon nanotubes are highly aromatic systems. Replacing one-half of the C atoms in CNTs by Si atoms decreases the aromaticity of each six-membered ring. The

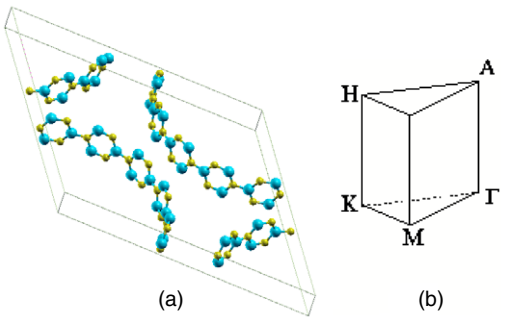

Figure 1. (Color online) (a) The unit cell of a (14, 14) SiCNT bundle. (b) The irreducible part of the hexagonal Brillouin zone for a crystalline bundle.

decreasing of aromaticity leads to the decrease in stability. Therefore, the exterior surface of SiCNTs has a higher reactivity than that of SWCNTs. For example, the electronic structures of SiCNTs can be manipulated by selected hydrogenation [8], and SiH_3 and CH_3 radicals can also be chemically adsorbed on the SiC nanotubes to form acceptor or donor levels, depending on the adsorption sites [9]. The differences between CNTs and SiCNTs also might give rise to clearly different interaction behaviors in each bundle.

Experimental and theoretical investigations have shown that SWCNTs in a bundle may deform from the ideal circular cross section of isolated tubes to a polygonized, hexagonal cross section [10, 11]. In this paper, for the first time, we investigate the structural characterizations and electronic properties of the bundles of polygonized SiCNTs using density functional theory (DFT) calculations. We have chosen large-diameter armchair (13, 13) and (14, 14) SiC nanotubes, with diameters of 22.3 and 23.97 Å, respectively.

Initially, we evaluate the variations of inter-tube interaction energy and geometrical structure of the SiCNTs arranged in a triangular lattice in the bundling process. We find a metastable structure and a highly stable structure corresponding to the circular and nearly hexagonal cross sections. By analyzing the band structures, the effects of polygonization on the electronic properties will also be discussed. This paper is organized as follows. In section 2 the computational model and method are presented. Section 3 contains results and discussion. The final section is the conclusion.

2. Computational model and method

The original SiCNT crystalline bundles could be modeled using a hexagonal primitive unit cell containing 26 Si and 26 C atoms for the (13, 13) bundle, and 28 Si and 28 C atoms for the (14, 14) bundle. Figures 1(a) and (b) show the unit cell and first Brillouin zone of a (14, 14) SiCNT bundle.

The total energy and electronic band structure calculations are performed via first-principles full potential linearized augmented plane-wave density functional theory, as implemented in the WIEN2K code [12]. For the exchange and correlation terms, the generalized gradient approximation (GGA) [13] is used. The core states are the 1s electrons of C and up to the 2p electrons for Si. Muffin-tin radii are 1.3 and 1.85 au for C and Si atoms, respectively. The number of k points in the whole Brillouin zone is taken to be equal to 200. The calculations were performed for the bundles of (13, 13) and (14, 14) SiC nanotubes. The optimizations were carried out with respect to both the atomic coordinates and the lattice constants, using the PORT method (a reverse-communication trust-region quasi-Newton method from the PORT library). Structural optimizations converge when the forces acting on each atom were smaller than 0.01 eV $Å^{-1}$.

3. Results and discussion

3.1. Structural characterization

We first obtained the equilibrium configurations of isolated SiCNTs. The calculated Si–C bond length is about 1.79 Å, which is in agreement with other *ab initio* results [7]. Similar to boron nitride (BN) nanotubes [14], the more electronegative C atoms moved radially outward from the tube axis and the more electropositive Si atoms moved in the opposite direction after relaxation, resulting in a buckled surface. Thus, the radial geometry of the tubular structures is characterized by two concentric cylindrical tubes, all the Si atoms forming the inner cylinder and all of the C atoms forming the outer cylinder. The radial buckling is defined by [15]

$$\beta = r_{\mathrm{C}} - r_{\mathrm{Si}} \tag{1}$$

where r_{C} and r_{Si} are the mean radii of the C and Si cylinders, respectively. The values of the radial buckling for (13, 13) and (14, 14) tubes are 0.04 and 0.037 Å, respectively. We define the diameter of the SiCNT as the average diameters of the Si ring and C ring. The calculated average diameter is 22.3 Å for (13, 13) SiCNT and it is 23.97 Å for (14, 14) SiCNT. The optimized lattice constant (L) along the tube axis is 3.11 Å for these SiCNTs.

Each of the SiC tubes in a bundle interacts with its six neighboring tubes. Here the inter-tube interaction energy per atom is defined by

$$E_I = E_{\mathrm{t-b}}(\text{nanotube in the bundle}) - E_{\mathrm{t-i}}(\text{isolated tube}) \tag{2}$$

where $E_{\mathrm{t-b}}$ (nanotube in the bundle) and $E_{\mathrm{t-i}}$ (isolated tube) are the total energy per atom of a SiC nanotube in the bundle and an isolated SiCNT, respectively. Figure 2 shows the inter-tube interaction energy as a function of the in-plane lattice constant a for the (14, 14) SiCNT bundle where both the atomic coordinates and the size of the hexagonal unit cell were optimized at each value of the in-plane lattice constant a. As shown in figure 2 there is a metastable minimum and a highly stable minimum in the inter-tube interaction energy curve, corresponding to a lattice of cylindrical tubes with little deformation and a lattice of SiCNTs having nearly hexagonal cross sections, respectively. The inter-tube interaction energy per atom at the most stable configuration is −26 meV, while it is −19 meV at the metastable configuration. For this large-diameter SiCNT the lattice of nearly hexagonal tubes

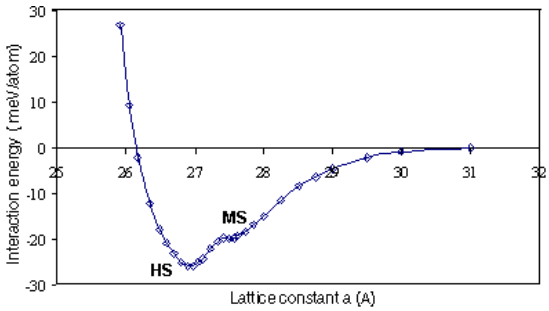

Figure 2. (Color online) The inter-tube interaction energy as a function of the in-plane lattice constant a for the (14, 14) SiCNT bundle. The metastable minimum and highly stable minimum are labeled as MS and HS, respectively.

is more stable than the one of circular tubes because of increased interfacial geometry between adjacent tubes. The inter-tube interaction energy curve shows that the energy barrier which is encountered in the bundling process is very small. This suggests that the polygonization of bundled SiCNTs may be a spontaneous procedure. We found that both optimized structures have approximately the same inter-tube spacing of 3.5 Å, which is larger than the inter-tube spacing of carbon nanotube bundles obtained within the same calculational framework [16, 17]. This result is related to the decreased aromaticity of SiCNTs with respect to the CNTs, giving rise to a weak π-stacking ability with another SiCNT in the bundle. Similarly, multi-walled SiCNTs differ significantly from the MWCNT geometries since the interlayer spacings are significantly larger than the 3.4 Å normally observed for the MWCNTs. The interlayer spacing ranges are from 3.8 to 4.5 Å in multi-walled SiCNTs [5]. This indicates very loose coupling between the layers [6]. The in-plane lattice constant a of the triangular lattice is given by the sum of the tube width (i.e. the tube diameter in the case of circular tubes and the distance between opposite faces of a tube in the case of hexagonal tubes) and inter-tube spacing. Since the diameter of a circular tube is larger than the distance between the opposite faces of the corresponding hexagonal tube, the cell parameter of the lattice of hexagonal tubes is smaller than the one of circular tubes. The calculated in-plane lattice constant a is 27.48 Å for the metastable structure and it is 26.97 Å for the minimum-energy structure. The density of the lattice of circular tubes is 1.52×10^{13} tubes cm^{-2} and the maximum bundle density would be up to 1.58×10^{13} tubes cm^{-2} for the lattice of nearly hexagonal tubes. The calculated inter-tube interaction energy per atom at the lowest energy configuration of a lattice of (13, 13) SiCNTs is -22 meV. Its value is slightly smaller than that of a lattice of (14, 14) SiCNTs. The cross section of a (14, 14) SiCNT in the bundle has a more polygonized shape compared with the (13, 13) SiCNT bundle (see figures 3(a) and (b)).

In contrast to the CNTs, there is a charge transfer from the Si to C in individual SiCNTs [18]. The charge density distribution for the (14, 14) SiCNT bundle is illustrated by the contour plot in figure 4(a). The charge density is strongly accumulated around the C atoms and there is no total charge density distribution between the tubes, as shown

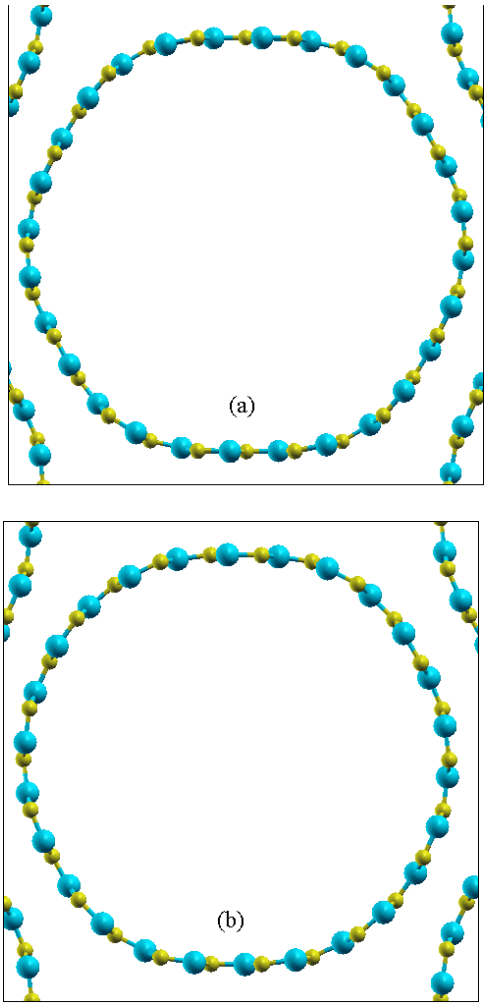

Figure 3. (Color online) Square slices of the cross sections of the lattices of (a) (14, 14) and (b) (13, 13) SiCNTs at the most stable configuration.

in figure 4(a). The charge density distribution for the two facing Si–C bonds with the same symmetry (for instance, two Si–C bonds indicated by arrows in figure 4(a)) in the plane perpendicular to the tubular axis of the bundled SiCNT are similar, while it is slightly different for the asymmetric Si–C bonds. This is because the inter-tube interactions along the six interacting directions would not be the same in the (14, 14) SiCNT bundle (see figure 4(b)).

3.2. Electronic properties

To understand how the electronic properties of large-diameter SiCNTs change when the tubes are bundled into ropes we first compare the band structure of an isolated (14, 14) SiCNT to that of the lattice of nearly hexagonal (14, 14) SiCNTs. Then we compare the band structure of the lattices of (14, 14) SiCNTs with nearly hexagonal and circular cross sections to study the effect of polygonization on the electronic properties of SiCNTs in the bundle. The calculated electronic band structure of the isolated (14, 14) SiCNT, shown in figure 5(a), indicates the (14, 14) SiCNT is an indirect-gap semiconductor

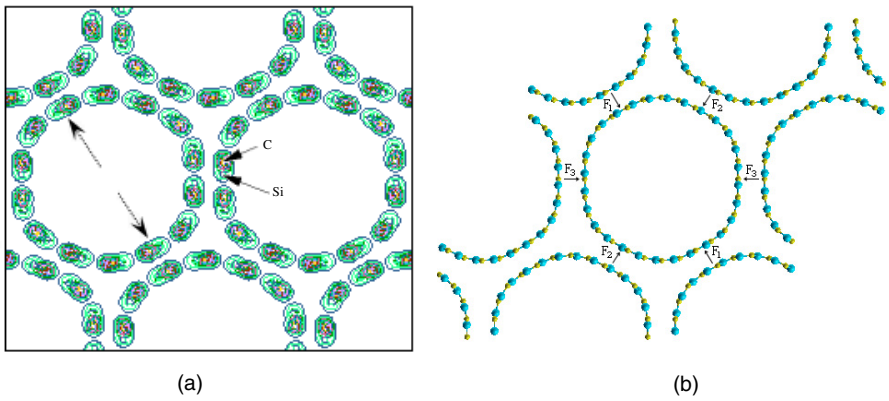

Figure 4. (Color online) (a) Contour plot of charge density distribution in a plane perpendicular to the tube axes of the most stable configuration of a lattice of (14, 14) SiCNTs. The arrows indicate two Si–C bonds with the same symmetry. (b) Force diagram of the (14, 14) SiCNT bundle. The arrows mean the directions of inter-tube interactions between SiCNTs.

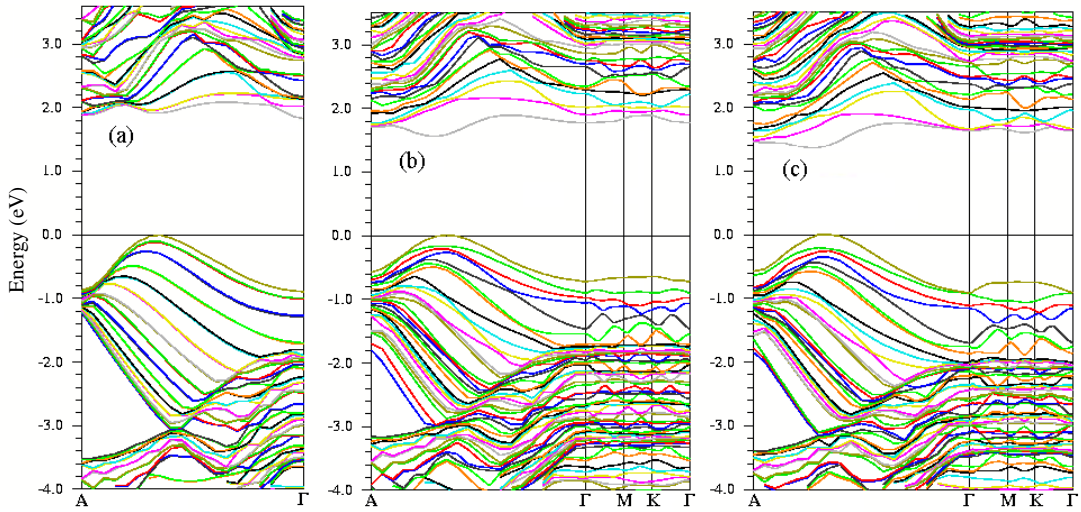

Figure 5. (Color online) Band structures of (a) isolated (14, 14) SiCNT along the tube axis and the lattices of (b) nearly hexagonal and (c) circular (14, 14) SiCNTs along the A–Γ–M–K–Γ symmetry directions of the first Brillouin zone.

where the bottom of the conduction band is at the Γ point and the top of the valence band is at about $0.65\frac{\pi}{L}$ in the (0, 0, 1) direction. The calculated bandgap is 1.82 eV, which is consistent with the previous calculational case [7]. Figure 5(b) shows the band structure of the lowest energy configuration of a lattice of (14, 14) SiCNTs corresponds to nearly hexagonal SiCNTs, along the A–Γ–M–K–Γ symmetry directions of the first Brillouin zone. By comparing the band structures of the isolated (14, 14) SiCNT (figure 5(a)) and the lattice of nearly hexagonal (14, 14) SiCNTs (figure 5(b)) along the tube axis from A to Γ a number of differences are evident: (i) the doubly degenerate bands in the isolated (14, 14) SiCNT split into non-degenerate states in the bundle; (ii) the bottom of the conduction band moves to $0.69(0, 0, 1)\frac{\pi}{L}$ from the Γ point, and the indirect bandgap decreases to 1.55 eV; and (iii) the valence and conduction bands are significantly expanded. All differences should be attributed to the inter-tube interactions that occur in the bundle. The interaction between the SiCNTs in the bundle does not only change the band structure along the tube's axis but causes the dispersion in the plane perpendicular to the tubular axis. The perpendicular dispersion leads to a broadening of the density of states in bundled tubes.

The effect of *polygonization* on the electronic properties of a (14, 14) SiCNT bundle is easily seen by comparing the band structures along the A–Γ–M–K–Γ symmetry directions of the first Brillouin zone for the most stable configuration and metastable configuration of the lattice of (14, 14) SiCNTs corresponding to the lattices of nearly hexagonal and circular (14, 14) SiCNTs, respectively (see figures 5(b) and (c)).

We observe that the dispersion of the occupied bands of the lattice of nearly hexagonal (14, 14) SiCNTs is larger than that of the lattice of circular (14, 14) SiCNTs. This is an effect of the increased interfacial geometry between adjacent tubes in the lattice of nearly hexagonal (14, 14) SiCNTs with respect to the lattice of circular (14, 14) SiCNTs, giving rise to a larger inter-tube coupling in the lattice of nearly hexagonal (14, 14) SiCNTs than in the lattice of circular (14, 14) SiCNTs. An increase in the bandgap by 0.18 eV is another notable effect of polygonization (see figures 5(b) and (c)).

4. Conclusion

In this paper, for the first time, we have reported results of *ab initio* calculations of the structural and electronic properties of bundles of large-diameter armchair SiCNTs. We have found that the cross sections of these large-diameter SiCNTs in the bundle have nearly hexagonal shape. The ground-state inter-tube separations and the maximum bundle densities were calculated for these large-diameter SiCNT bundles. The inter-tube spacing of the large-diameter SiCNT bundles is found to be larger than that of the CNT bundles. We studied the effect of bundling on the electronic band structure of the isolated (14, 14) SiCNT. Our electronic structure calculations show that the inter-tube coupling leads to the splitting of the doubly degenerated states, reduction of the bandgap and the expansions of valence and conduction bands. Our results show that the polygonization of the SiCNTs in the bundle leads to a further dispersion of the occupied bands. Another notable effect of polygonization is an increase in the bandgap by 0.18 eV.

References

[1] Iijima S 1991 *Nature* **345** 56
[2] Dai H 2002 *Surf. Sci.* **500** 218
[3] Dresselhaus M S, Dresselhaus G and Eklund P C 1996 *Science of Fullerenes and Carbon Nanotubes* (San Diego, CA: Academic)
[4] Moradian R, Azadi S and Rafii-Tabar H 2007 *J. Phys.: Condens. Matter* **19** 176209
[5] Sun X H, Li C P, Wong W K, Wong N B, Lee C S, Lee S T and Teo B K 2002 *J. Am. Chem. Soc.* **124** 14464
[6] Menon M, Richter E, Mavrandonakis A, Froudakis G and Andriotis A N 2004 *Phys. Rev.* B **69** 115322
[7] Zhao M, Xia Y, Li F, Zhang R Q and Lee S T 2005 *Phys. Rev.* B **71** 085312
[8] Zhao M, Xia Y, Zhang R Q and Lee S T 2005 *J. Chem. Phys.* **122** 21470
[9] Li F, Xia Y Y, Zhao M W, Liu X D, Huang B D, Yang Z H, Ji Y J and Song C 2005 *J. Appl. Phys.* **97** 104311
[10] Lopez M J, Rubio A, Alonso J A, Qin L C and Iijima S 2001 *Phys. Rev. Lett.* **86** 3056
[11] Tersoff J and Ruoff R S 1994 *Phys. Rev. Lett.* **73** 676
[12] Blaha P, Schwarz K, Madsen G K H, Kvasnicka D and Luitz J 2001 *WIEN2K* Vienna University of Technology, Austria ISBN 3-9501031-1-2
[13] Perdew J P, Burke S and Ernzerhof M 1996 *Phys. Rev. Lett.* **77** 3865
[14] Menon M and Srivastava D 1999 *Chem. Phys. Lett.* **307** 407
[15] Baumeier B, Kruger P and Pollmann J 2007 *Phys. Rev.* B **76** 085407
[16] Moradian R, Behzad S and Azadi S 2008 *Physica* E **40** 3055
[17] Reich S, Thomsen C and Ordejon P 2002 *Phys. Rev.* B **65** 155411
[18] Mavrandonakis A, Froudakis G E, Schnell M and Muhlhauser M 2004 *Nano Lett.* **3** 1481